Talanta 216 (2020) 120966

Contents lists available at ScienceDirect

Talanta

journal homepage: www.elsevier.com/locate/talanta

A novel ligase chain reaction-based electrochemical biosensing strategy for highly sensitive point mutation detection from human whole blood

Zhou-Jie Liu[a,1], Liang-Yong Yang[a,1], Qing-Xia Wei[a], Chen-Liu Ye[b], Xiong-Wei Xu[a], Guang-Xian Zhong[a], Yan-Jie Zheng[b], Jin-Yuan Chen[a,**], Xin-Hua Lin[b,***], Ai-Lin Liu[b,*]

[a] Department of Pharmacy, Central Laboratory, Fujian Provincial Key Laboratory of Precision Medicine for Cancer, First Affiliated Hospital of Fujian Medical University, Fuzhou 350005, China

[b] Department of Pharmaceutical Analysis, Higher Educational Key Laboratory for Nano Biomedical Technology of Fujian Province, Faculty of Pharmacy, Fujian Medical University, Fuzhou 350122, China

ARTICLE INFO

Keywords:
Electrochemical biosensor
Point mutation
*CYP2C19*2* allele
Ligase chain reaction
Clinical sample

ABSTRACT

Challenged by the detection of trace amounts of mutants and disturbance from endogenous substances in clinical samples, herein, we present a novel electrochemical biosensor based on ligase chain reaction (eLCR) via the thermostable ligase with high mutation recognizing ability. The lengthened double-stranded DNAs exponentially generated via LCR were uniformly distributed on a bovine serum albumin-modified gold electrode, in which the phosphate buffer was tactfully added to remove adsorbed uninterested-probes, and thereafter the amperometry current was collected for the specific binding of streptavidin-poly-HRP and subsequent catalysis in the 3, 3′, 5, 5′-tetramethylbenzidine substrate that contained hydrogen peroxide. It found that, under optimized conditions, the proposed biosensor exhibited a high selectivity of mutant targets from the 10^4-fold excess of co-existent wild targets within a detection limit of 0.5 fM. Impressively, without the involvement of pre-PCR, the homozygous mutants were specifically distinguished from the wild genotype of *CYP2C19*2* allele in human whole blood samples. Therefore, the proposed eLCR, due to its advantages in simple primer design, operational ease and ease of miniaturization, has demonstrated its considerable potential for point-of-care testing in the diagnosis of point mutation-related diseases and personalized medicine.

1. Introduction

Increasing evidence has revealed that single-nucleotide polymorphisms (SNPs), also known as point mutations, are valuable genetic markers for cancer diagnosis and prognosis [1,2], and important predictors of drug efficacy [3] and drug resistance [4,5]. However, accurate detection of SNPs is extremely demanding, as the impact of a single variable nucleotide on the properties of a target sequence is limited. Besides, real-world samples are usually composed of subtle quantities of mutants and excessive amounts of wild-type genes, leading to the difficulty in selectively identifying a SNP in the presence of a large excess of the wild-type genes (> 100 fold).

In detecting SNPs, PCR-based [6,7] and sequencing-related [8] technologies are mostly applied, but these methods, due to their labour intensity and cost, and limited detection of rare point mutations, fall short of qualified routine diagnostic tools. Currently, several new, more suitable designs are employed to make possible sensitive detection of point mutations based on specifically designed hybridization probes [9,10], mutation recognizing enzymes [11–13] and thermal denaturation [14]. Therein, ligation-based SNP assays are most attractive for their superiority in selectivity over other assays, especially the ligase chain reaction (LCR) [15], in which the target DNA and ligated probes are simultaneously amplified in the presence of mutants during thermal cycling, resulting in sensitive assays whilst maintaining specificity.

As LCR is a useful technology to achieve allelic discrimination and its amplification efficiency is comparable to that of PCR, the development of a readout method, well suited for routine clinical use and coupled to LCR, is highly desired. Notably, Wang et al. have developed a single quantum dot (QD)-based multiplexed coincident fluorescence detection method with an outstanding performance in the detection of

* Corresponding author.
** Corresponding author.
*** Corresponding author.
E-mail addresses: cjyfjmu@163.com (J.-Y. Chen), xhl1963@sina.com (X.-H. Lin), ailinliu@fjmu.edu.cn (A.-L. Liu).
[1] These authors contributed equally to this work.

https://doi.org/10.1016/j.talanta.2020.120966
Received 11 December 2019; Received in revised form 21 March 2020; Accepted 23 March 2020
Available online 29 March 2020
0039-9140/

point mutations by combining Gap-LCR and QD-single molecule spectroscopy [16]. However, this system required cumbersome and expensive instrumentation, which is not appropriate for point-of-care (POC) analysis. Compared with fluorescent [16], optical [17,18], mass [19]-based methods, the electrochemical method [20,21] has inherent advantages of portability, simplicity, rapidity, and inexpensiveness, so the development of an alternative strategy, which is electrochemistry-based and highly amenable to POC, can therefore make a significant impact in clinical practice. Previously, Wee et al. have transformed the LCR-based electrochemical biosensor (eLCR) by using conventional macro-disk electrodes [22] into a microdevice-based sensor platform [23]. This platform, however, still involves pre-PCR in real sample assay of cell lines and purified serum DNA. It employed a classic modification method with subsequent self-assembled DNA, backfilling with 6-mercapto-1-hexanol, hybridization with LCR products, and incubation in streptavidin-HRP solution, in which, due to the close proximity to the interface, it was difficult to obtain a hybridization efficiency approximating that in homogeneous solution, resulting in a limited sensitivity. More recently, Easley et al. proposed a nucleic acid nanostructure for electrochemical detection of a broad range of analytes through on-electrode ligation [24], which demonstrates that the ligated DNA nanostructure comprising an electrochemical label is more stable than its hybrid form, implying the being-easy disturbance of electrochemical labels introduced via noncovalent DNA hybridization.

Inspired by the above-mentioned findings, we herein presented a robust eLCR for sensitive, rapid and low-cost detection of clinically important single DNA base change by immobilising the generated dsDNA products into a BSA-based porous monolayer, which possesses improved sensitivity, stability and operational ease. Rather than introducing the electrochemical label via noncovalent DNA hybridization, as mostly traditional electrochemical methods do, the proposed strategy integrated the anchor unit-thiol and the binding moiety-biotin into a single stable entity. Specially, this protocol was designed on the following bases: (1) the rapid assembly of dsDNA can be realized by the stronger assembly capacity of dsDNA, owing to its rigid structure and easier access to inter-protein pores than ssDNA [25]; (2) a BSA-based DNA probe carrier offered by our group [26] was employed for a better controlling of inter-probes and subsequently effective binding of streptavidin-HRP; (3) as a new strategy, phosphate buffer (PB) was added into the amplified products to inhibit unwanted DNA probes from being adsorbed on the gold electrode, mainly via the phosphate backbone and partly due to bases [27], so as to improve the signal-to-noise ratio of this biosensor.

CYP2C19, as an important human drug metabolism gene, is responsible for metabolizing commonly-used drugs, including clopidogrel, proton pump inhibitors (PPIs), etc. *CYP2C19*1* is a wild-type allele that encodes an enzyme for its normal activity whereas *CYP2C19*2*, an important mutant site in the *CYP2C19* gene occurring at G681A, encodes an inactive enzyme, resulting in poor metabolism. Genotyping of this SNP in *CYP2C19* has been approved for application in clinical pharmacogenomics testing and personalized medicines [28] and is herein used for the verification of this proposed biosensor in the real-world samples. As a result, the proposed scheme successfully achieved detection of point mutation, *CYP2C19*2* as our target gene, without the involvement of pre-PCR, and homozygous wild (*CYP2C19*1*1*) together with homozygous mutant (*CYP2C19*2*2*) were directly distinguished in the total nucleic acid extracted from human whole blood samples. This assay may have potential to serve as an alternative for point mutation detection in the clinical practice.

2. Experimental sections

2.1. Materials and reagents

The Ampligase® thermal stable ligase and 10 × reaction buffer [200 mM Tris-HCl (pH 8.3), 250 mM KCl, 100 mM $MgCl_2$, 5 mM NAD, and 0.1% Triton® X-100] were purchased from Epicenter Technologies (Madison, USA). Bovine serum albumin (BSA) was obtained from Shanghai Sangon Biological Engineering Technology and Services Co., Ltd. (Shanghai, China). The 3, 3′, 5, 5′-tetramethylbenzidine (TMB) substrate [Enhanced K-blue substrate, hydrogen peroxide (H_2O_2) included] was from Neogen (Lansing, USA). Salmon sperm DNA and streptavidin-poly-horseradish peroxidase (SA-poly-HRP) were purchased from Thermo Fisher Scientific (Waltham, USA). The phosphate buffers (PB) (a mixture of 10 mM Na_2HPO_4 and NaH_2PO_4) (pH 7.4) used in this study were as follows: 10 mM PB as washing buffer and 0.2 M PB as inhibiting buffer.

Oligonucleotides used in this study were synthesized and PAGE-purified by TaKaRa Biotechnology Co., Ltd. (Dalian, China), and the sequences of *CYP2C19*2* (rs4244285) were listed as follows (from 5′ to 3′, the underlined base representing one mutant site):

Wild target (WT):

TTCCCACTATCATTGATTATTTCCCGGGAACCCATAACAAATTACTTAAAA

Mutant target (MT):

TTCCCACTATCATTGATTATTTCCCAGGAACCCATAACAAATTACTTAAAA

Ligated probe (LP);

T_{10}TTTAAGTAATTTGTTATGGGTTCCTGGGAAATAATCAATGATAGTGGGAA

Half mutant target 1 (MT-1): TTCCCACTATCATTGATTATTTCCCA-OH

Half mutant target 2 (MT-2): PO_4-GGAACCCATAACAAATTACTTAAAA

Capture probe (CP): SH-$(CH_2)_6T_{10}$TTTAAGTAATTTGTTATGGGTTCC-OH

Signal probe (SP): PO_4-TGGGAAATAATCAATGATAGTGGGAA-Biotin

All solutions were prepared with Milli-Q water (18 MΩ cm^{-1} resistivity) from a Millipore system. The other reagents were of analytical reagent grade and used without further purification.

2.2. Clinical sample collection and human genomic DNA extraction

The human whole blood samples were collected from the Pharmacy Department of the First Affiliated Hospital of Fujian Medical University. This study strictly followed the ethical guidelines of the Declaration of Helsinki and was approved by the Ethics Committee for Human Research, the First Affiliated Hospital of Fujian Medical University. The human genomic DNA was extracted in an automatic magnetic bead extraction and purification system (Pre-NT, Perkin Elmer) according to the instructions, and quantified from the absorption at 260 nm with a Nanodrop 2000 (Thermo Scientific). Sequencing of the *CYP2C19*2* was determined by TaKaRa Inc. (Dalian, China).

2.3. Homogeneous ligase chain reaction

The LCR was conducted in a 50 μL of reaction volume containing 10 × reaction buffer, 2 U ampligase, 20 nM of the four probes (CP, SP, MT-1, MT-2), and various amounts of mutants and/or wild type template (synthetic DNA or genomic DNA extracted from the whole blood). The mixture was first incubated at 94 °C for 5 min, and then a 30-cycle thermal cycling was conducted at 45 °C for 60 s, 53 °C for 60 s, and 94 °C for 60 s. After the thermal cycling, a 2.5 μL volume of 0.2 M PB (pH 7.4) was added into the amplified solution. Thereafter, ligation products were stored at room temperature (RT, 25 °C) to ensure the formation of dsDNA until use.

2.4. Construction of the dsDNA-BSA-based biosensing platform

Firstly, the gold electrode (2 mm in diameter) was physically polished and electrochemically treated following the reported protocol

[29]. Then, the cleaned electrode was immersed in 10 mM PB (pH 7.4) containing 0.1 mg mL^{-1} BSA at RT for 15 min. After washing with 10 mM PB, the BSA modified electrode was incubated in the amplified solution containing 0.2 M PB at RT for 1 h, and then rinsed with the washing buffer and blow-dried with nitrogen. Subsequently, 3 μL volume of SA-poly-HRP (1:1000) was dropped onto the electrode surface and incubated at RT for 15 min. Finally, the electrode was extensively rinsed with ultrapure water and subjected to electrochemical measurements.

2.5. Electrochemical measurements

The amperometric experiment was performed on an electrochemical workstation (CHI 760D, Chenhua Co., Shanghai, China), which has a conventional Au disk working electrode, an Ag/AgCl reference electrode filled with saturated KCl solution, and a Pt wire auxiliary electrode. Amperometric detection was performed in TMB substrate at RT with the fixed potential set at 0.1 V and the electrocatalysis reduction current was measured at 100 s until the HRP redox reaction reached a steady state.

3. Results and discussion

3.1. Design and principle of the dsDNA/BSA monolayer-based eLCR for point mutation detection

The dsDNA/BSA monolayer-based eLCR strategy for the detection of point mutation in genomic DNA is schematically illustrated in Scheme 1. BSA molecules were firstly self-assembled on the gold electrode to form a porous monolayer, and then dsDNAs generated from LCR were inserted into gaps between BSAs via Au–S bond, resulting in uniform distribution of dsDNAs on BSA monolayer at a certain distance. In this study, point mutation of *CYP2C19*2* allele was employed as the model where the base pair at the SNP site was A/T in the mutant DNA and G/C in the wild DNA. Herein, four probes (CP, SP, MT-1, MT-2) were designed, among which MT-1 and MT-2 were halved from the MT, while CP and SP were respectively complementary to MT-2 and MT-1. Specifically, CP was labeled with SH at its 5′ terminal for immobilization; SP and MT-2 were labeled with PO_4 at their 5′ terminals for ligation; the 3′ terminal of SP was labeled with biotin for coupling with SA-poly-HRP as a source of electrocatalysis reduction current. At the first stage, when the perfectly base-paired hybridization between two probes (CP and SP) and one template MT occurred at 45 ˚C, the 3′-OH of CP was immediately adjacent to the 5′-PO_4 of the SP, forming a nicked duplex which was subsequently filled with a phosphodiester bond generated by the ampligase's catalysis at 53 ˚C. However, the ligation was not triggered in the wild target, due to the presence of single-base mismatch at the nicked site. At the second stage of 94 ˚C, all of the DNA strands were melted and freed as single strands. Therefore, under the thermal cycling, the template MT was cyclically used in one ligation, and the ligated product in turn became the template for subsequent ligation, so the ligation products were exponentially generated, leading to the generation of abundant dsDNAs with modified ends (SH group and biotin label) after repeated thermal cycles. Afterwards, the rigid dsDNAs were inserted into the gaps of BSA through the Au–S bond. Then, SA-poly-HRPs were specifically bound to the biotin labels via the biotin-avidin bridge. Finally, the target DNA was quantified by detecting the electric current generated by poly-HRP-catalyzed reduction of H_2O_2 contained in the TMB substrate.

3.2. Electrochemical detection and characterization of native polyacrylamide gel electrophoresis

Amperometry was employed as means of quantitative measurement. As shown in Fig. 1A, an increasing curve for current (I) versus time (T) was observed instantly after the onset of the potential (~0.1 V), which reached a plateau (steady-state current) within ~100 s. Indeed, in the presence of 10 fM WT (curve b), only a relatively small and stable amperometric current (~318 nA) was observed, which was close to the current (~245 nA) in the absence of the target DNA (curve a), while the amperometric current (~1478 nA) for 10 fM MT (curve c) was significantly larger than both of them. These results evidence the feasible discrimination between WT and MT, which is due to the employment of LCR amplification and TMB-H_2O_2-HRP system.

In order to demonstrate the ligation products generated in the presence of MT, native polyacrylamide gel electrophoresis (PAGE, 15%) was applied to identify the electrophoretic mobility of different DNA products. As shown in Fig. 1B, lane 1 and 2 were respectively used for the PAGE analysis of LCR products with and without MT. According to the marker bands on the right lane M, the front band was caused by the remaining SP/MT-1 (26 bp) and CP/MT-2 (25 bp), which fully matched the band in lane 4 containing a mixture of SP, MT-1, CP and MT-2. As expected, a slower band in lane 1 was observed, indicating the formation of the ligated duplex of the secondary target/biotinyl-ligated capture probe in the presence of MT. However, the position of this slower band in lane 1 did not match that of lane 3 containing hybrids between LT and MT, which may be attributed to the binding of ampligase at the ligation site in the duplex DNA structure, leading to the decreased mobility. Altogether, these findings suggest that the LCR has been successfully promoted by the MT.

3.3. The critical effect of phosphate on the suppression of nonspecific adsorption of DNA probes

As specified, the LCR was performed in the provided 1 × reaction buffer. Unfortunately, a high background current was obviously observed in the absence of the target DNA (as shown in the left group of Fig. 2), hindering the sensitivity of the biosensor. In order to obtain a high signal-to-noise ratio, factors, such as nonspecific adsorption of SA-poly-HRP and DNA probes, and nonspecific amplification, were considered. The results showed that the adsorption of DNA probes on the gold electrode greatly contributed to the background current. As shown in the right group of Fig. 2, in the LCR products, the presence of SP alone produced a current as high as 2240 nA, which was immediately reduced to 246 nA without SP, indicating that the adsorption of biotin-labeled SP onto the gold electrode and subsequent binding of SA-poly-HRP lead to the generation of a high current. Of note, the current in the column of SP + PB was almost reduced to that of the column without SP, suggesting that a complete desorption is achieved by adding PB into the LCR products. Importantly, the response from the blank group was reduced by adding 2.5 μL volume of 0.2 M PB into 50 μL LCR products, while the response from the target group with PB approximated that without PB (as shown in the middle group of Fig. 2). The desorption mechanism may be explained by the fact that, due to the adsorption of phosphate ions, the surface of the gold electrode is negatively charged [30], resulting in an electrostatic repulsion to DNA strands. It is worth noting that the existed nonthiolated dsDNAs (SP and MT-1) in the LCR products will enhance the adsorption of the DNA probes on the gold electrode, for the phosphate backbone of dsDNAs is more easily exposed to the solution than that of ssDNAs [31], indicating the essential coexistence of PB.

3.4. Analytical performance of the proposed eLCR for point mutation detection

3.4.1. Optimization of the experimental conditions

In order to obtain an optimal biosensor performance, the key experimental parameters such as hybridization/ligation temperature and amount of ampligase were examined and optimized. Given the time cost, the thermal cycle number of the LCR was fixed at 30 [32,33].

In the stage of hybridization/ligation, the partial probes were hybridized with the target DNA, producing a nick for the recognition and

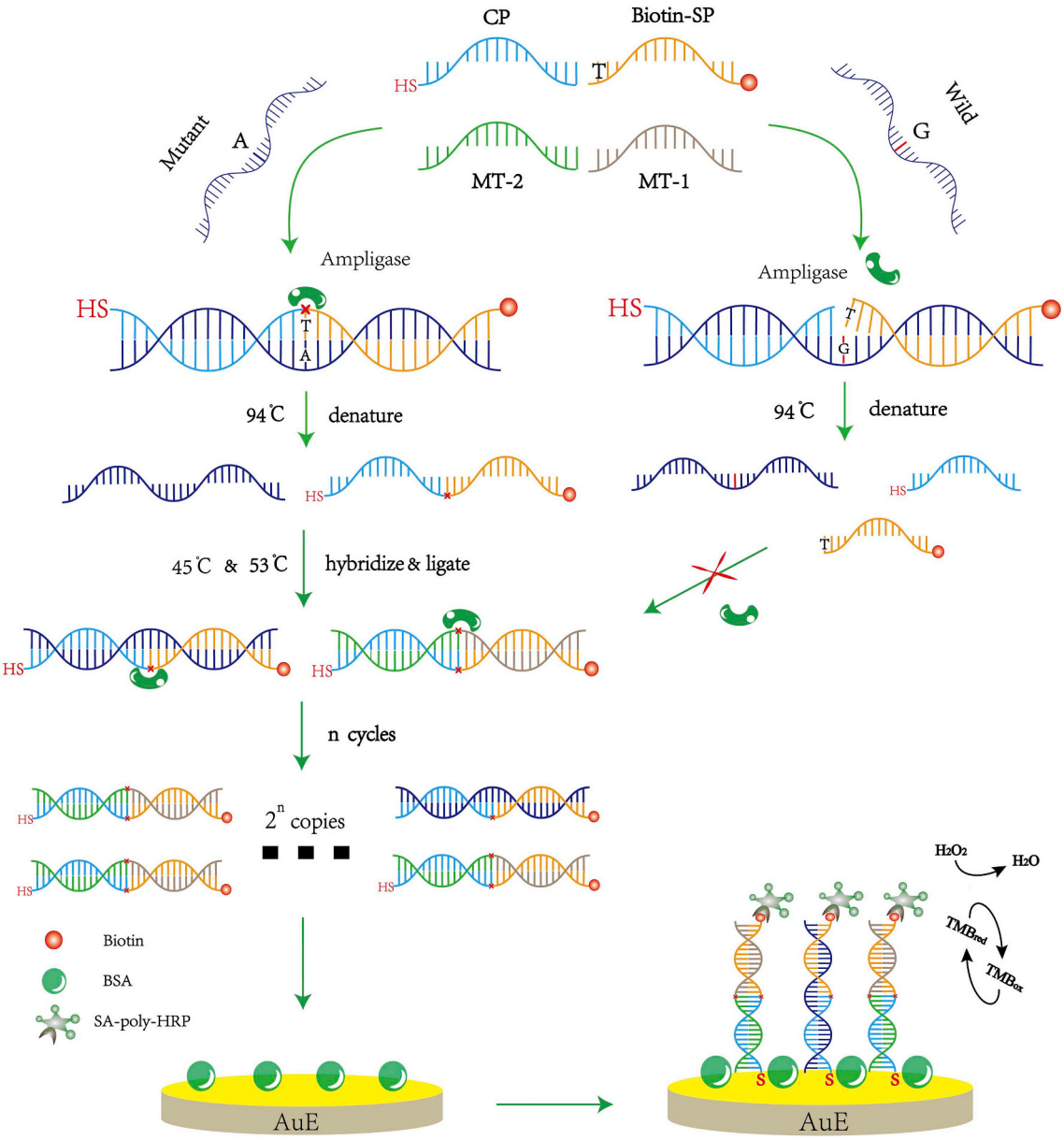

Scheme 1. Schematic illustration of the LCR-based electrochemical biosensor via dsDNA-BSA platform for point mutation detection. LCR process: Initially, the mutant target hybridizes perfectly with probe CP and SP, forming a nicked duplex, then the nick is ligated by ampligase. Afterwards, the thermal-cycle setting makes denature-hybridize-ligate perform with the participation of CP, SP, MT-2. MT-1, so the ligation products would be exponentially generated. However, the hybridization between wild target and probes, due to one-base mismatch, forms a defective nicked-duplex that could not be fully recognized by ampligase, losing the ability to trigger this LCR process.

catalysis of ampligases, so an optimal temperature was crucial for effective hybridization and high activity of the ampligase. As shown in Fig. S2, the amperometric current increased significantly from 45 °C to 53 °C and decreased obviously afterwards. Traditionally, only one temperature point at the peak of the curve was set in this stage. However, results from Fig. S3 demonstrated, for the first time, a division of 45 °C for 2 min or 53 °C for 2 min into 45 °C for 1 min and then 53 °C for 1 min greatly enhanced the amplification efficiency, indicating that the division operation can guarantee a full hybridization and subsequent ligation. Therefore, 45 °C/53 °C was selected for subsequent experiments.

During the LCR, sufficient ampligase was needed to complete the ligation reaction in a short time. As shown in Fig. S4, the current response from 1 pM MT paralleled the increasing amount of the ampligase (from 0.5 U to 2 U) and then flattened, while the current response from 1 pM WT significantly arose from 2 U. Therefore, 2 U of the ampligase was employed in the following experiments to get the maximum difference between MT and WT.

3.4.2. Sensitivity and selectivity of the proposed eLCR

Under the optimal condition, the MT targets at various concentrations were analyzed using the proposed eLCR. As shown in Fig. 3A, the current response decreased with the declining concentrations of MT and approximated that of the blank group (curve a, ~249 nA) at 0.5 fM (curve b, ~353 nA), which was estimated as the limit of detection ($> 3\sigma$). As shown in Fig. 3B, the plot of the amperometric response vs. the logarithm of MT concentration (from 10 fM to 100 pM) showed a strong linear relationship with a correlation coefficient of 0.9963, spanning approximately 4 orders of magnitude. Obviously, these results indicate that this proposed electrochemical biosensor is highly sensitive, as a result of the high amplification efficiency of LCR, dsDNA assembling on the BSA-based carrier platform, and effective inhibition of

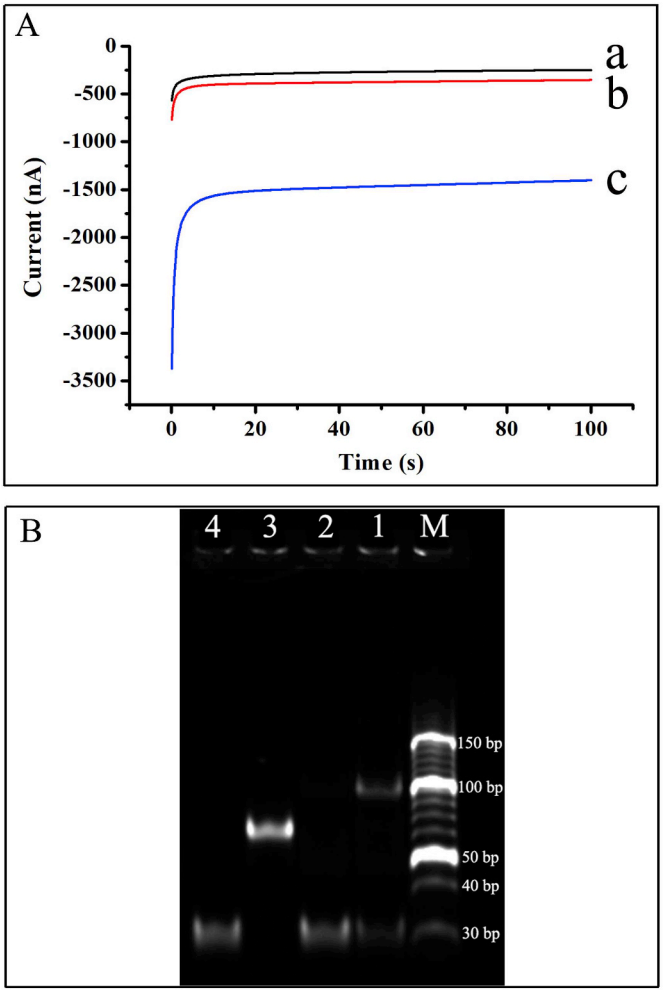

Fig. 1. (A) Comparison of the amperometric response among blank (a), 10 fM WT (b), 10 fM MT (c). (B) 15% native-PAGE analysis of different DNA solutions. Lane M: 150 bp DNA ladder; Lane 1: the LCR products in the presence of 10 nM MT; Lane 2: the LCR products in the absence of MT; Lane 3: the mixture of LT and MT; Lane 4: the mixture of SP, MT-1, CP and MT-2. The concentration of probes used was 1 μM. The electrophoresis was performed in 1 × Tris-borate-EDTA (TBE) buffer at 100 V for 2 h.

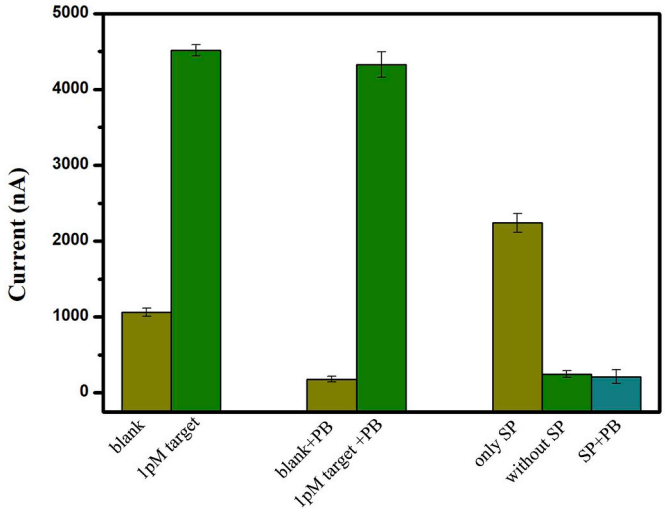

Fig. 2. Comparison of amperometric response in different LCR components with or without PB. Mean values and standard deviations are obtained from five independent experiments.

the nonspecific adsorption of DNA probes by PB regulation. In addition, on the basis of five independent measurements of 1 pM MT with five different electrodes, the relative standard deviation (RSD) was estimated to be 7.8%, indicating the good precision of this eLCR.

To demonstrate the high selectivity of this biosensor for point mutation detection in real-world samples, it is necessary to evaluate its ability to detect trace amounts of MTs in the presence of a large quantity of WTs. Herein, the ratios of WT to MT from 1:1 to 10000: 1 were examined with the concentration of the WT fixed at 10 pM. As shown in Fig. 3C, even when the ratio of WT to MT was as high as 10000:1 (1 fM MT), the current response was still distinguished from that of 10 pM WT (1:0), indicating a high specificity toward MT and a promising application prospect.

3.4.3. Anti-interference analysis in simulated samples

The anti-interference analysis was conducted by mixing the target DNA with salmon sperm genomic DNA, which is similar to the human genome DNA [34] and commonly used as the simulated sample. Usually, the concentration of extracted genomic DNA from human whole blood sample was from 10 ng μl^{-1} to 100 ng μl^{-1}, measured by Nanodrop 2000, so different concentrations of salmon sperm genome DNA (5 ng μl^{-1}, 10 ng μl^{-1}, 20 ng μl^{-1}, 30 ng μl^{-1}, 50 ng μl^{-1}, 100 ng μl^{-1}, 200 ng μl^{-1}) with 1 μl volume were chosen to investigate their interfering effects. As shown in Fig. 4A, the amperometric response (1 pM MT) failed to respond to the addition of the salmon sperm genomic DNA before its concentration exceeded 20 ng μl^{-1}, which was also observed when other concentrations were administered. Results from Fig. 4B showed the amperometric current from 20 ng salmon sperm genomic DNA was approximate to the background current, demonstrating the suitability of salmon sperm genome DNA as the simulated sample. Besides, the current response from spiked MT in 20 ng salmon sperm genomic DNA was close to that from pure MT, indicating the high anti-interference ability of this eLCR. Therefore, in real sample assay, the added quantity was fixed at 20 ng so that every measured sample had the same concentration but produced no interference on the proposed biosensor.

3.5. Real sample assay for *CYP2C19*2* allele genotyping

The human whole blood samples were collected from the Pharmacy Department of the First Affiliated Hospital of Fujian Medical University and their genotypes of *CYP2C19*2* allele were determined using DNA microarray chip. For electrochemical detection, ten *CYP2C19*1/*1* samples, ten *CYP2C19*2/*2* samples and ten *CYP2C19*1/*2* samples were randomly selected. After extraction and measurement by Nanodrop 2000, they were added into the LCR solution with a final quality of 20 ng and then underwent the proposed eLCR. As shown in Fig. 5A, the currents (693 nA–1228 nA) obtained from *CYP2C19*2*2* samples were significantly higher than those (300 nA–400 nA) from *CYP2C19*1*1* samples, with 20 ng salmon sperm genomic DNA as control, while the current response from *CYP2C19*1*2* was not distinguished from that of *CYP2C19*2*2* and *CYP2C19*1*1*. These results suggest that the large number of uninterested DNAs in the real-world samples, as well as the residual reagents in the DNA extraction process, do not affect the sensitivity of this eLCR method. Moreover, sequencing analysis (Fig. 5B) further confirmed our results. Collectively, these results provide comprehensive evidence that the proposed eLCR can be applied for point mutation detection of *CYP2C19*2* allele in clinical samples with a high sensitivity and selectivity, demonstrating its considerable potential in the diagnosis of SNP-related diseases diagnosis and personalized medicine.

To better show the advantages of the proposed eLCR, the performance of this method was compared with the other biosensors for *CYP2C19*2* allele determination in terms of experimental period, ratio (mutant vs. wild), and real sample type. As shown in Table S1, the experimental period of this biosensor was significantly shortened,

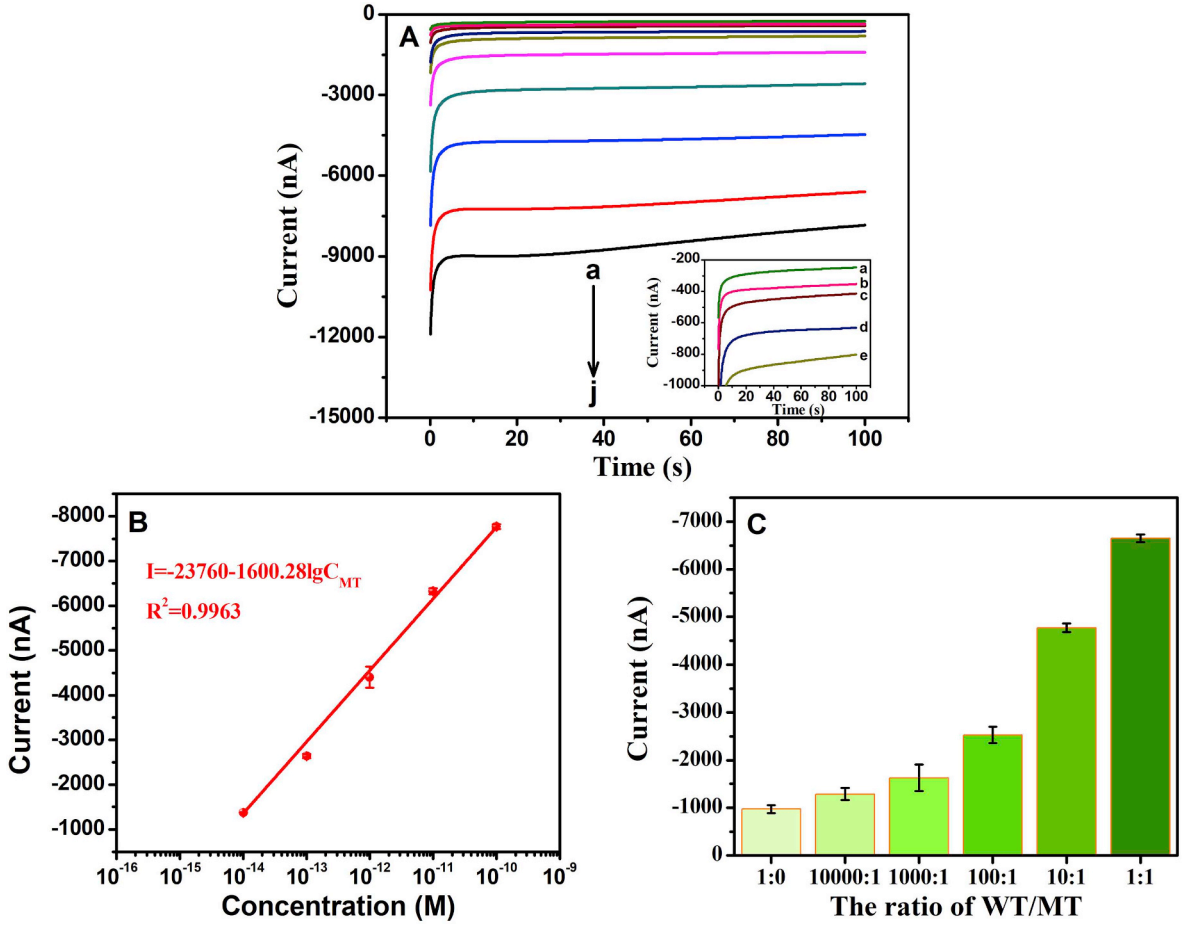

Fig. 3. (A) Amperometric curves of MT with a series of concentrations (a→j: 0, 0.5 fM, 0.6 fM, 0.8 fM, 1 fM, 10 fM, 100 fM, 1 pM, 10 pM, 100 pM) in TMB substrate. (B) Calibration plot of the amperometric current versus logarithmical concentration of the MT (from 1.0×10^{-15} M to 1.0×10^{-10} M). (C) Comparison of current response from different ratios of WT/MT (1:0, 1:1, 10:1, 100:1, 1000:1, 10000:1), where the concentration of the WT was fixed at 10 pM. Error bars show the standard deviations of measurements taken from three independent experiments (n = 3).

which can be attributed to the strategy of dsDNA assembling on the BSA-based carrier platform. Moreover, the proposed biosensor detected a much lower ratio of MT/WT (0.01%) and realized a direct detection of DNA extract from clinical blood sample without the involvement of pre-PCR. In this regard, our proposed method not only matches these methods in detection performance but also has notable advantages in terms of design simplicity and operational ease.

4. Conclusion

The current study provides a novel eLCR for highly sensitive point mutation detection by coupling the strategy of dsDNA assembling on

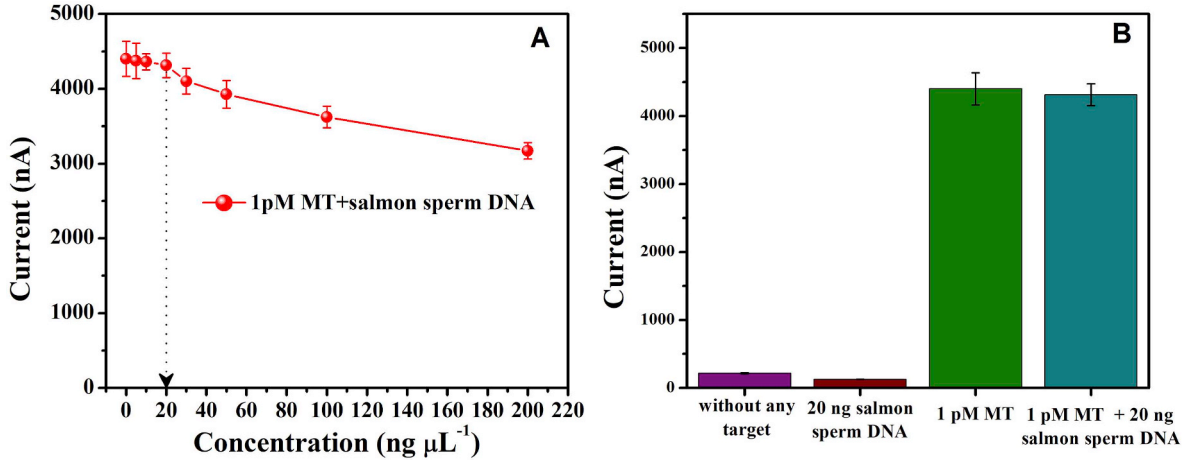

Fig. 4. (A) Current response from 1 pM MT spiked with different concentration of the salmon sperm DNA (0, 5 ng μl^{-1}, 10 ng μl^{-1}, 20 ng μl^{-1}, 30 ng μl^{-1}, 50 ng μl^{-1}, 100 ng μl^{-1}, 200 ng μl^{-1}). (B) Comparison of current response from different samples (without any target, 20 ng salmon sperm DNA, 1 pM MT, 1 pM MT + 20 ng salmon sperm DNA). Error bars show the standard deviations of measurements taken from three independent experiments (n = 3).

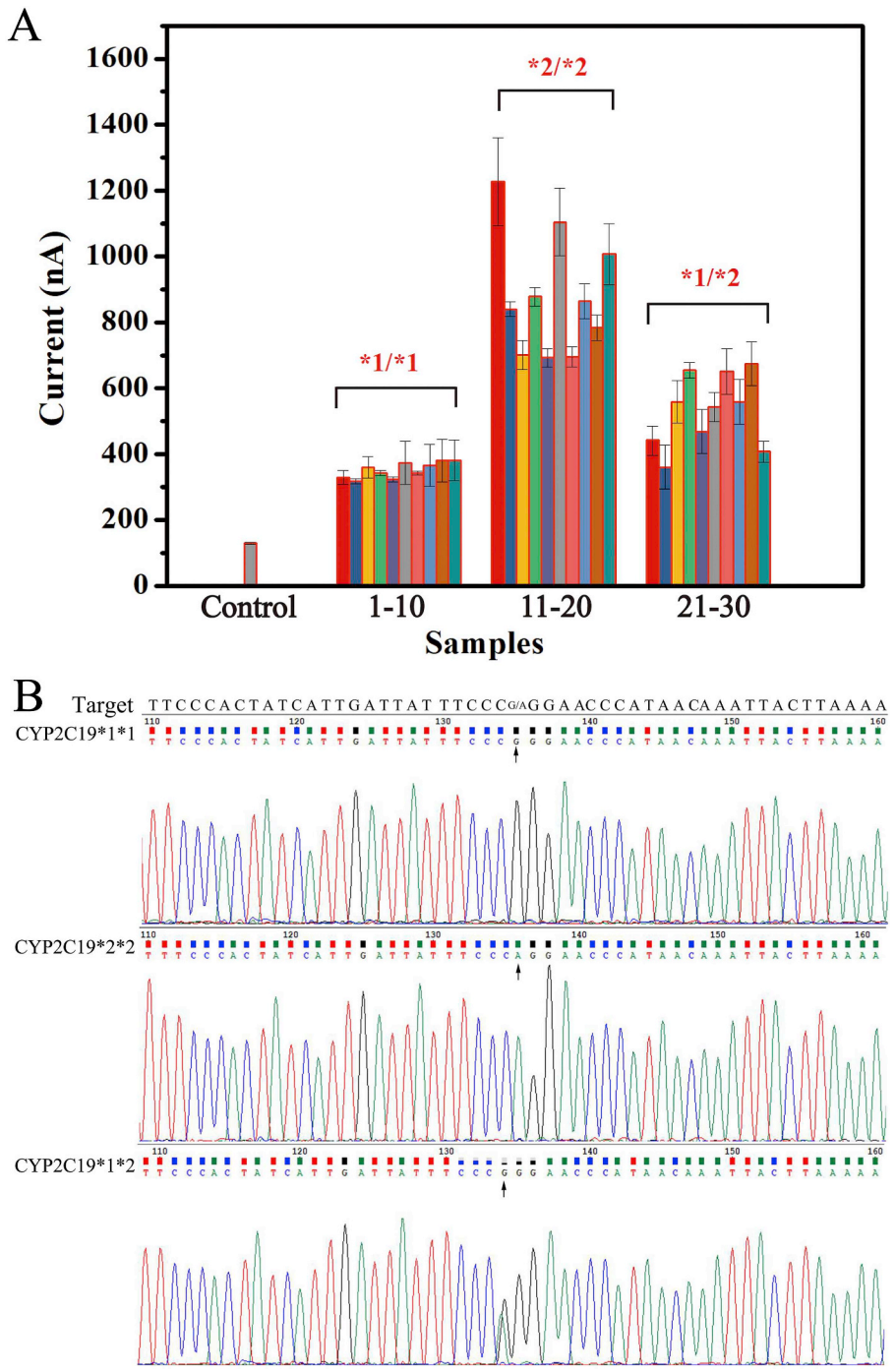

Fig. 5. (A) Amperometric response of the biosensor to the real clinical samples. Error bars show the standard deviations of measurements taken from three independent experiments in each sample. (B) Graph matching gene sequencing of three real samples selected from each group. Arrows indicate the mutational sites.

the BSA-based carrier platform with PB regulation-induced inhibition of nonspecific adsorption of DNA probes. Significantly, the point mutation of *CYP2C19*2* allele can be directly distinguished without the involvement of pre-PCR in real-world samples, which indicates a universal application for genomic DNA detection and demonstrates its profound clinical significance in diagnosis of microbial infection and SNP-related disease.

CRediT authorship contribution statement

Zhou-Jie Liu: Investigation, Writing - original draft. **Liang-Yong Yang:** Investigation, Writing - original draft. **Qing-Xia Wei:** Investigation. **Chen-Liu Ye:** Investigation. **Xiong-Wei Xu:** Investigation. **Guang-Xian Zhong:** Investigation. **Yan-Jie Zheng:** Investigation. **Jin-Yuan Chen:** Project administration, Writing - review & editing. **Xin-Hua Lin:** Project administration, Supervision. **Ai-Lin Liu:** Project administration, Writing - review & editing.

Declaration of competing interest

The authors declare that they have no known competing financial interests or personal relationships that could have appeared to influence the work reported in this paper.

Acknowledgments

This work was financially supported by the National Natural Science Foundation of China (21775023, 21705021); the Medical Elite Cultivation Program of Fujian Province (2018-ZQN-49); the Medical Innovation Project of Fujian Province (2016-CX-44); Social Development Guiding Programs of Fujian Province of China (2019Y0012); the Startup Fund for Scientific Research, Fujian Medical University (2017XQ1057); and the Special Fund of Youth Top-Notch Innovative Talents of Fujian Province (SQNBJ201601).

Appendix A. Supplementary data

Supplementary data to this article can be found online at https://doi.org/10.1016/j.talanta.2020.120966.

References

[1] D. Sidransky, Emerging molecular markers of cancer, Nat. Rev. Cancer 2 (2002) 210–219.
[2] C.L. Ho, R.J. Kurman, R. Dehari, T.L. Wang, I.M. Shih, Mutations of BRAF and KRAS precede the development of ovarian serous borderline tumor, Cancer Res. 64 (2004) 6915–6918.
[3] J.C. Soria, Y.L. Wu, K. Nakagawa, S.W. Kim, J.J. Yang, M.J. Ahn, J.C. Yang, Y. Lu, S. Atagi, Gefitinib plus chemotherapy versus placebo plus chemotherapy in EGFR-mutation-positive non-small-cell lung cancer after progression on first-line gefitinib (IMPRESS): a phase 3 randomised trial, Lancet Oncol. 16 (2015) 990–998.
[4] T.J. Price, M. Peeters, T.W. Kim, J. Li, S. Cascinu, P. Ruff, A.S. Suresh, A. Thomas, S. Tjulandin, K. Zhang, S. Murugappan, R. Sidhu, Panitumumab versus cetuximab in patients with chemotherapy-refractory wild-type KRAS exon 2 metastatic colorectal cancer (ASPECCT): a randomized, multicentre, open-label, non-inferiority phase 3 study, Lancet Oncol. 15 (2014) 569–579.
[5] F. Coll, J. Phelan, G.A. Hill-Cawthorne, M.B. Nair, K. Mallard, S. Mallard, A.M. Abdallah, S. Alghamdi, M. Alsomali, A.O. Ahmed, Genome-wide analysis of multi- and extensively drug-resistant mycobacterium tuberculosis, Nat. Genet. 50 (2018) 307–316.
[6] L. Zhou, R.A. Palais, C.N. Palais, K.B. Geiersbach, C.T. Wittwer, Copy number assessment by competitive PCR with limiting deoxynucleotide triphosphates and high-resolution melting, Clin. Chem. 61 (2015) 724–733.
[7] J.S. Farrar, C.T. Wittwer, Extreme PCR: efficient and specific DNA amplification in 15-60 seconds, Clin. Chem. 61 (2015) 145–153.
[8] D. Aggeli, V.O. Karas, N.A. Sinnott-Armstrong, V. Varghese, R.W. Shafer, W.J. Greenleaf, G. Sherlock, Diff-seq: a high throughput sequencing-based mismatch detection assay for DNA variant enrichment and discovery, Nucleic Acids Res. 46 (2018) e42.
[9] H.N. Bengtson, S. Homolka, S. Niemann, A.J. Reis, S.P. Da, Y.V. Gerasimova, D.M. Gerasimova, K.H. Rohde, Multiples detection of extensively drug resistant tuberculosis using binary deoxyribozyme sensors, Biosens. Bioelectron. 94 (2017) 176–183.
[10] S. Hu, N. Li, F. Liu, Combining cooperativity with sequestration: a novel strategy for discrimination of single nucleotide variants, Chem. Commun. (Camb.). 54 (2018) 3223–3226.
[11] Z. Zhang, I. Hsing, Nucleic acid self-assembly circuitry aided by exonuclease III for discrimination of single nucleotide variants, Anal. Chem. 89 (2017) 12466–12471.
[12] Y. Huang, Y.L. Zhang, X. Xu, J.H. Jiang, G.L. Shen, R.Q. Yu, Highly specific and sensitive electrochemical genotyping via gap ligation reaction and surface hybridization detection, J. Am. Chem. Soc. 131 (2009) 2478–2480.
[13] E.S. Yamanaka, L.A. Tortajada-Genaro, N. Pastor, Á. Maquieira, Polymorphism genotyping based on loop-mediated isothermal amplification and smartphone detection, Biosens. Bioelectron. 109 (2018) 177–183.
[14] B.V. Grinsven, N.V. Bon, H. Strauven, L. Grieten, M. Murib, K.L.J. Monroy, S.D. Janssens, K. Haenen, M.J. Schöning, V. Vermeeren, Heat-transfer resistance at solid-liquid interfaces: a tool for the detection of single-nucleotide polymorphisms in DNA, ACS Nano 6 (2012) 2712–2721.
[15] W. Shen, H. Deng, H. Gao, Gold nanoparticle-enabled real-time ligation chain reaction for ultrasensitive detection of DNA, J. Am. Chem. Soc. 134 (2012) 14678–14681.
[16] Y. Song, Y. Zhang, T.H. Wang, Single quantum dot analysis enables multiplexed point mutation detection by gap ligase chain reaction, Small 9 (2013) 1096–1105.
[17] J.H. Kim, J.E. Park, M. Lin, S. Kim, G.H. Kim, S. Park, G. Ko, J.M. Nam, Sensitive, quantitative naked-eye biodetection with polyhedral Cu nanoshells, Adv. Mater. 29 (2017) 1702945.
[18] A. Nano, A.N. Boynton, J.K. Barton, A rhodium-cyanine fluorescent probe: detection and signaling of mismatches in DNA, J. Am. Chem. Soc. 139 (2017) 17301–17304.
[19] J.H. Park, H. Jang, Y.K. Jung, Y.L. Jung, I. Shin, D.Y. Cho, H.G. Park, A mass spectrometry-based multiplex SNP genotyping by utilizing allele-specific ligation and strand displacement amplification, Biosens. Bioelectron. 91 (2017) 122–127.
[20] S. Park, J.E. Jeong, V.S. Le, J. Seo, B. Yu, D.Y. Kim, S.H. Kwon, S. Jon, H.Y. Woo, H. Yang, Enhanced electron transfer mediated by conjugated polyelectrolyte and its application to washing-free DNA detection, J. Am. Chem. Soc. 140 (2018) 2409–2412.
[21] J. Das, I. Ivanov, T. Safaei, E. Sargent, S.O. Kelley, Combinatorial probes for high-throughput electrochemical analysis of circulating nucleic acids in patient samples, Angew. Chem. Int. Ed. Engl. 57 (2018) 3711–3716.
[22] E.J. Wee, M.J. Shiddiky, M.A. Brown, M. Trau, eLCR: electrochemical detection of single DNA base changes via ligase chain reaction, Chem. Commun. (Camb.). 48 (2012) 12014–12016.
[23] E.J. Wee, S. Rauf, K.M. Koo, M.J. Shiddiky, M. Trau, μ-eLCR: a microfabricated device for electrochemical detection of DNA base changes in breast cancer cell lines, Lab Chip 13 (2013) 4385–4391.
[24] S. Somasundaram, C.J. Easley, A nucleic acid nanostructure built through on-electrode ligation for electrochemical detection of a broad range of analytes, J. Am. Chem. Soc. 141 (2019) 11721–11726.
[25] Y.H. Liu, H.H. Deng, H.N. Li, T.F. Shi, H.P. Shi, A.L. Liu, W. Chen, G.L. Hong, A DNA electrochemical biosensor based on homogeneous hybridization for the determination of cryptococcus neoformans, J. Electroanal. Chem. 827 (2018) 27–33.
[26] Y.H. Liu, H.N. Li, W. Chen, A.L. Liu, X.H. Lin, Y.Z. Chen, Bovine serum albumin-based probe carrier platform for electrochemical DNA biosensing, Anal. Chem. 85 (2013) 273–277.
[27] X. Zhang, F. Wang, B.W. Liu, E.Y. Kelly, M.R. Servos, J.W. Liu, Adsorption of DNA oligonucleotides by titanium dioxide nanoparticles, Langmuir 30 (2014) 839–845.
[28] C.L. Zhang, J.L. He, Y.C. Zhang, J. Chen, Y.L. Zhao, Y.Z. Niu, C. Yu, Cerium dioxide-doped carboxyl fullerene as novel nanoprobe and catalyst in electrochemical biosensor for amperometric detection of the *CYP2C19*2* allele in human serum, Biosens. Bioelectron. 102 (2018) 94–100.
[29] D. Jambrec, F. Conzuelo, B. Zhao, W. Schuhmann, Potential-pulse assisted thiol chemisorption minimizes non-specific adsorptions in DNA assays, Electrochim. Acta 276 (2018) 233–239.
[30] H.X. Li, L.J. Rothberg, Label-free colorimetric detection of specific sequences in genomic DNA amplified by the polymerase chain reaction, J. Am. Chem. Soc. 126 (2004) 10958–10961.
[31] X. Zhang, M.R. Servos, J.W. Liu, Surface science of DNA adsorption onto citrate-capped gold nanoparticles, Langmuir 28 (2012) 3896–3902.
[32] W. Shen, H.M. Deng, A.K.L. Teo, Z.Q. Gao, Colorimetric detection of single-nucleotide polymorphisms with a real-time PCR-like sensitivity, Chem. Commun. 48 (2012) 10225–10227.
[33] Y.Q. Cheng, J.J. Zhao, H.L. Jia, Z. Yuan, Z.P. Li, Ligase chain reaction coupled with rolling circle amplification for high sensitivity detection of single nucleotide polymorphisms, Analyst 138 (2013) 2958–2963.
[34] A. Castro, R.T. Okinaka, Ultrasensitive, direct detection of a specific DNA sequence of bacillus anthracis in solution, Analyst 125 (2000) 9–11.